Engineering Research Express

PAPER • **OPEN ACCESS**

Numerical search for time-of-flight focusing conditions and its application to the analysis of TOF mass analyzer schemes

To cite this article: Zhanar Kambarova *et al* 2024 *Eng. Res. Express* **6** 015037

Engineering Research Express

PAPER

Numerical search for time-of-flight focusing conditions and its application to the analysis of TOF mass analyzer schemes

Zhanar Kambarova[1,*], **Arman Saulebekov**[2] and **Andrey Trubitsyn**[3]

[1] Buketov Karaganda University, Universitetskaya str. 28, Karaganda 100026, Kazakhstan
[2] Lomonosov Moscow State University, Kazakhstan branch, Kajimukan str.11, Astana 010010, Kazakhstan
[3] Ryazan State Radio Engineering University named after V.F. Utkin, Gagarina str. 59/1 Ryazan 390005, Russia
[*] Authors to whom any correspondence should be addressed.

E-mail: kambarova@bk.ru, saulebekov@mail.ru and assur@bk.ru

Keywords: charged particle optics, corpuscular-optical system, time-of-flight focusing, time-of-flight charged particle mass analyzer, electron mirror

OPEN ACCESS

RECEIVED
17 August 2023

REVISED
15 December 2023

ACCEPTED FOR PUBLICATION
8 January 2024

PUBLISHED
17 January 2024

Abstract

A method of searching for high-order time-of-flight focusing conditions based on data of numerical trajectory analysis of corpuscular-optical systems is presented. The method makes it possible to determine the maximum achievable order of focusing, the value of the independent variable (initial coordinate, initial angle, initial velocity or energy) relative to which the focusing is observed, as well as the spatial position of focus. The method has been tested on model problems. The corpuscular-optical properties of time-of-flight devices with known analytical solutions are investigated, and the uniqueness of their parameters in their class is shown.

Introduction

The time-of-flight analysis of ion packets from the source to the collector is a recently mastered practical method that underlies the operation of most modern mass spectrometers [1]. However, time-of-flight analyzers have a much wider scope of application than commonly believed. For example, the mechanism of time-of-flight separation of electrons can be used in the construction of photoelectron spectrometers [2].

In work [3], a possible application of the time-focusing Time-of-Flight (tfTOF) method in combination with energy filters was investigated for the Karlsruhe Tritium Neutrino experiment KATRIN [4]. The study demonstrated that the tfTOF method can be used in general and in particular to modify the sensitivity to certain energy and angular characteristics of a charged particle source. Additionally, TOF analyzers can be used as an additional element of cameras [5] with wide instantaneous viewing angle to measure ion masses in the study of energy and angular distributions of hot space plasma.

Devices with very different electrode configurations (linear drift, post-source pulse focusing TOF mass analyzers, single and double-stage mirror linear-reflectron with normal and oblique incidence, cylindrical mirror, single and multiple spherical sector and poloidal electrostatic deflectors) are used to study the time-of-flight characteristics of charged particle flows [6]. Linear time-of-flight mass spectrometers (TOFMS), which have been around for over 50 years [7], are still used in practice and have been further developed [8]. It is well-known that using multi-field linear TOFMS can improve the analyzer parameters due to the higher-order spatial focusing relative to the initial ion position [9]. In this case, the focusing conditions in linear TOFMS are traditionally determined using simple analytical formulas.

A much better mass resolution is provided by the use of ion mirrors in the so-called mass reflectrons, whose role is reduced to compensation of the time of flight for ions with different initial energies [10, 11]. In the simplest single-stage mass reflectrons with a grid electrode at the input, it is possible to fulfill the conditions for the first-order time-of-flight focusing by energy [10]. More complex two-stage reflectrons have the property of the second-order time-of-flight focusing and they are used with a significant energy spread of ions [12]. The main parameters of mass reflectrons are limited by the processes of ion scattering on input grids. It is worth

noting that grid mass reflectrons allow the searching of time-of-flight focusing conditions based on an analytical approximation.

Efficient reflectron designs without a grid were proposed in the 1980s, consisting of three coaxial cylindrical electrodes of the same diameter [13]. In work [14], the possibility of implementing first-order spatial-time-of-flight focusing in a two-electrode mirror of rotational symmetry for two regimes with large and small drift distances was shown for the first time. The numerical-analytical technique [14] for searching for the conditions for spatial-time-of-flight focusing in electrostatic mirrors, formed by several successive cylinders of the same radius, was further developed in [15]. The aberration coefficients in such mirrors are expressed by certain integrals and evaluated numerically at each step of integration of the differential equation of the paraxial trajectory. Since the turning point of the trajectory in mirrors has zero potential, the formulas for calculating the aberration coefficients are similar to the known formulas for cathode lenses. This work proves the implementation of up to third-order time-of-flight focusing by energy.

By now, ion mirrors have become an integral part of the most advanced mass spectrometric equipment, such as Q-TOF mass spectrometers [16]. Q-TOF mass spectrometers combine TOF and quadrupole instruments, a pairing that results in high mass accuracy for precursor and product ions, strong quantitation capability, and fragmentation experiment applicability.

In electron optics, the quality of focusing is determined by aberrations, which are deviations from the paraxial approximation. There are no aberration-free systems. One of the main problems in corpuscular optics is to identify the types of aberrations inherent in a given system and then to eliminate or reduce the most objectionable ones. Despite the quality of time-of-flight focusing being the main determinant of the parameters of time-of-flight analyzers, there are currently no general approaches to establishing the conditions and level of time-of-flight focusing for devices of arbitrary design. The purpose of this work is to fill this gap. In summary, the proposed method answers the following questions:

- whether a simulated (arbitrary design) corpuscular-optical system can provide high- quality time-of-flight focusing;
- what is the value of the initial parameter (spatial position of the particle source center, central initial angle, central initial energy), near which high-quality time-of-flight focusing is ensured;
- where to place the particle collector in order to meet the conditions for high-quality time-of-flight focusing.

Mathematical description of focusing quality

The focusing properties of corpuscular-optical systems can be described in terms of aberration theory - improvement of these properties is possible only by reducing aberration coefficients.

It is more convenient to measure some parameters characterizing particles not relative to zero, but relative to the corresponding parameters of the reference particle, which is sometimes called central one. The parameters of this particle denoted by the superscript *(ref)*. In each profile plane perpendicular to the z-axis, an arbitrary particle in a beam is characterized by the following parameters [17]:

- x and y coordinates;
- angular coordinates $a = tg\alpha = dx/dz = p_x/p_z$ and $b = tg\beta = dy/dz = p_y/p_z$ in x and y directions, respectively; here α and β are initial angles with respect to x and y, p_x, p_y and p_z are components of the momentum along the Cartesian axes;
- divergence in the time of flight $T = t - t^{(ref)}$ (measured from some initial profile plane) of the considered particle and the reference particle;
- relative deviation $\delta = (K/q - K^{(ref)}/q^{(ref)})/(K^{(ref)}/q^{(ref)})$ of the ratio of kinetic energy K to charge q for the considered particle with respect to the reference particle;
- relative deviation $\gamma = (m/q - m^{(ref)}/q^{(ref)})/(m^{(ref)}/q^{(ref)})$ of the ratio of mass m to charge q for the considered particle with respect to the reference particle.

The motion of an arbitrary particle is completely described by its position vector: $\boldsymbol{X}(z) = (x(z),\ a(z),\ y(z),\ b(z),\ T(z),\ \delta(z),\ \gamma(z))$. Like all other components, the time component of the position vector $\boldsymbol{X}(z)$ can be written as a function of the initial parameters $x, a, y, b, z, T, \delta, \gamma$, marked with the subscript «0», i.e. $T(z) = T(x_0, a_0, y_0, b_0, z_0, T_0, \delta_0, \gamma_0; z)$. The expansion of the T function in a power series (called the aberration expansion) with respect to the initial parameters has the following form

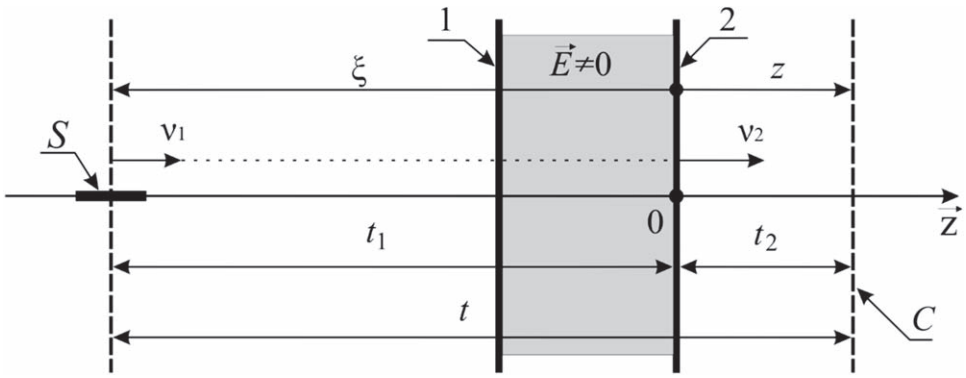

Figure 1. Search for conditions of time-of-flight focusing with respect to the initial coordinate on the z -axis: $\xi = z$.

$$\begin{aligned} T(z) = {} & (T|x)x_0 + (T|a)a_0 + (T|y)y_0 + (T|b)b_0 \\ & + (T|z)z_0 + (T|T)T_0 + (T|\delta)\delta_0 + (T|\gamma)\gamma_0 \\ & + (T|xx)x_0^2 + (T|xa)x_0a_0 + (T|aa)a_0^2 + (T|xy)x_0y_0 \\ & + (T\,|\,xb)x_0b_0 + (T\,|\,xz)x_0z_0 + (T\,|\,x\delta)x_0\delta_0 \; + \; \ldots, \end{aligned}$$

where we use the notation of partial derivatives accepted in charged particle optics [18].

The quality of focusing in the profile plane z can be expressed by the norm of the $T(z)$ function, quantified, for example, as $m\alpha x\,[T(z)]$, the value of which is determined by the interference of all aberration coefficients. Note that ideal focusing occurs when $T(z) = t - t^{(ref)} = 0$, in which case all particles with different initial data cross the z -plane at the same time. To determine the degree of influence on focusing of the each position vector components, the focusing order should be studied in relation to that component.

Method formalization

Let us denote any of parameters x_0, a_0, y_0, b_0, z_0, T_0, δ_0 or γ_0 by ξ_0, with respect to the variation of which the time-of-flight focusing is studied. Then the time of arrival of the reference particle to the profile plane will be expressed as $t^{(ref)} = t(\xi_0)$, and the time of arrival of the considered particle as $t = t(\xi) = t(\xi_0 + \Delta\xi)$, where $\Delta\xi$ is the variation of the initial parameter ξ_0, $\xi = \xi_0 + \Delta\xi$. To simplify the presentation of the proposed method's mathematical and physical essence, we take the $\xi_0 = z_0$ initial position of the particle on the z -axis as an independent variable.

Mathematically, the time-of-flight focusing order is expressed by the quantity of zero total derivatives in the expansion of the time of a particle flight from a source S extended along the z-axis to a profile plane (collector C) (figure 1) in a Taylor series in the initial coordinates $\xi = \xi_0 + \Delta\xi$

$$t(\xi_0 + \Delta\xi) = t(\xi_0) + t' \quad (\xi_0)\Delta\xi + t'' \quad (\xi)\Delta\xi^2/2 + \ldots,$$

where ξ_0 is the central (unknown) coordinate of the source, relative to which the particles are focused on the collector in terms of the time of flight. The focusing order N occurs when $t' \quad (\xi_0) = t'' \quad (\xi_0) = \cdots = t^{(N)}(\xi_0) = 0$. The total derivatives of time t with respect t_0 the initial parameter ξ in the presented formulas are indicated by the corresponding number of dash lines, for example, $t'' \quad (\xi) = \left.\frac{d^2t}{d\xi^2}\right|_{\xi=\xi_0}$.

The movement time $t(\xi)$ of a particle with mass m, emitted from a source with a velocity v_1, can be expressed as the sum $t(\xi) = t_1(\xi) + t_2(\xi)$, where $t_1(\xi)$ is the time of movement from the S source to the output electrode 2; $t_2(\xi)$ is the time of movement in the fieldless space between electrode 2 and the collector C. In general, an electric field $\vec{E} \neq 0$ can be created between the input 1 and output 2 electrodes of the time-of-flight analyzer. Since $t_2(\xi) = z/v_2(\xi) = z{\cdot}\nu(\xi)$, where z is the (unknown) distance from the output electrode 2 to the collector C, the function $\nu(\xi) = 1/v_2(\xi)$, $v_2(\xi)$, is the velocity of the particle when it leaves the region of the non-zero field gradient, then the first-order focusing condition will look like this $t' \quad (\xi) = t_1' \quad (\xi) + t_2' \quad (\xi) = t_1' \quad (\xi) + z{\cdot}\nu'(\xi) = 0$ or

$$z = -t_1' \quad (\xi)/\nu'(\xi). \tag{1}$$

The second-order focusing condition (N = 2) will follow from the equality to zero of the second derivative of time t with respect to ξ and substitution into this equality of the first- order focusing condition (1), i.e. from

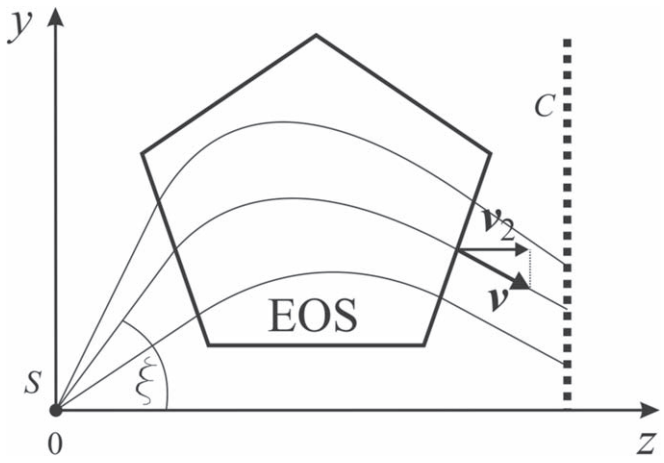

Figure 2. Search for conditions of time-of-flight focusing in an electron-optical system (EOS) with respect to the initial angle $\xi = \alpha$.

the equation $t''(\xi) = t_1''(\xi) + t_2''(\xi) = t_1''(\xi) + x{\cdot}\nu''(\xi) = t_1''(\xi) - t_1'(\xi){\cdot}\nu''(\xi)/\nu'(\xi) = 0$ or in a more convenient form

$$F(\xi) = t_1''(\xi){\cdot}\nu'(\xi) - t_1'(\xi){\cdot}\nu''(\xi) = 0. \tag{2}$$

The solution $\xi = \xi_0$ of the algebraic equation (2) determines the central coordinate of the source S extended along the z -axis, and (see equation (1)) the value

$$z = z_C = -t_1'(\xi_0)/\nu'(\xi_0) \tag{3}$$

is a collector position providing second-order time-of-flight focusing. It is obvious that focusing of order N in the plane $z = z_C$ will take place if the additional equalities

$$t_1^{(n)}(\xi_0){\cdot}\nu'(\xi) - t_1'(\xi_0){\cdot}\nu^{(n)}(\xi) = 0,\ n = 3, 4 \ldots N. \tag{4}$$

In the numerical analysis of the focusing properties of corpuscular-optical systems, in accordance with equation (2), the function $F(\xi)$ is formed on a limited discrete set of initial coordinates ξ_i of particle motion where the derivatives of the functions $\nu(\xi_i)$ and $t_1(\xi_i)$ are calculated using finite difference formulas. Then, the discrete function $F(\xi_i)$ is interpolated between any adjacent points, and equation (2) is solved numerically (e.g., by the dichotomy method) with respect to the central coordinate of the source $\xi = \xi_0$. After that, the position of the second-order focus (collector) $z = z_C$ is determined from Expression (3), and the conditions (4) of focusing of order $N > 2$ are checked.

To search for the conditions for time-of-flight focusing of an order higher than the second one, we recommend using the formalism of correlation analysis, which is described in detail in the author's work [19] as applied to the search for angular focusing and can be easily extended to the problem under study.

Furthermore, note that the method presented here can be extended to study the time-of-flight properties with respect to the remaining initial parameter, such as x_0, a_0, y_0, b_0, T_0, δ_0 or γ_0. As an example, figure 2 presents clarifying material for studying the time-of-flight properties of systems with a point source emitting particles at different initial angles α_0. In this case, the parameter ξ represents the initial angle of the particle motion, and the velocity v_2 is the projection of the velocity v of the particle onto the z -axis in the region where there is no potential gradient.

It should be noted that the time intervals t_1 and t_2 mentioned earlier were only introduced to simplify the understanding of the essence of the method, and when implementing the method, we only need data on the time duration t_1 of the each particle's movement from the source to some arbitrarily given surface in the region where there is no field gradient, as well as the projections v_2 of their velocities onto the normal to this surface. Such an arbitrary surface is the trajectory counting stop surface, and it is an essential component of any software application for modeling corpuscular-optical systems.

Spatial focusing refers to the focusing of charged particles in a plane perpendicular to the axis of the corpuscular-optical system. In axially-symmetric problems, such as those where the z -axis is the axis of symmetry. In this case, the order of spatial focusing is determined by the number N of first zero terms in the expansion of the arrival radius r on the ξ (initial particle position or angle). When $N > 1$, we have high-order spatial focusing. Spatial focusing is directly related to spherical aberrations of charged particle optics systems. Therefore, the physical principles of increasing the order of spatial focusing are based on the synthesis of fields,

that not only focusing but also compensate for the difference in motion conditions of particles that start with different initial data.

Testing and application of the method

The proposed method is algorithmized and integrated into the author's computer application 'FOCUS' [20]. In this application, the outer Dirichlet problem of potential theory is solved using the Boundary Elements Method (BEM). The advantage of this approach is that each electrode in the external setting can have an arbitrary thickness and complicate shape, which allows for simulating corpuscular-optical systems that are closer to real devices. Additionally, the Boundary Elements Method offers high computational speed due to the organization of multi-threaded calculations, with almost no additional 'overhead,' unlike other commonly used methods such as finite difference (FDM) and finite element methods (FEM). One of the main advantages of using the BEM in the software application for modeling corpuscular-optical systems is the possibility of studying multiscale designs including cathodes with small emission area, or electrodes of long length with small isolation gaps between them, etc.

In the software 'FOCUS', every i-th particle trajectory is calculated using numerical Runge–Kutta schemes. Numerical differentiation of the functions $\nu(\xi_i)$ and $t_l(\xi_i)$ is carried out according to finite-difference formulas on a five-point template. The software 'FOCUS' offers two modes of visualizing the results of trajectory analysis: continuous trajectories of all launched particles and the spatial position of these particles at discrete instants in time.

The proposed numerical method was tested on model problems.

The choice of the first example is based on the fact that, due to its infinite symmetry, a spherical capacitor is almost the main tool for testing software for modeling corpuscular-optics systems, both with respect to the accuracy of calculating the electrostatic field and the trajectories of charged particles in this field. What matters to us is, that in a spherical capacitor (figure 3) charged particles emitted along radial trajectories from a point source s located at the center of the spheres will return to the same center if their energy (in eV) is less than the potential difference between the inner 1 (radius $R_1 = 1$, potential is 0) and outer 2 (radius $R_2 = 2$, potential is 1) spheres. Moreover, the symmetry of problem implies the equivalence of the values of the return time to this point for all particles, i.e. ideal time-of-flight focusing will be observed at this point. In the test problem, particles with energy of 0.9 eV, 'launched' from the capacitor center s within the angle range of $10°-170°$, reached an equipotential with a potential value of 0.9 V, changed the direction of movement to the opposite one at a moment in time t_α (positions of particles at subsequent moments of time t_b, t_c, t_d, t_e are shown in figure 3) and, having flown through the center s (t_f is moment of time after passing the center s on figure 3), stopped moving in an arbitrarily given plane 3, perpendicular to the r-axis and located at an arbitrary given distance from the source s. Based on the results of calculations using the 'FOCUS' application, with an error in calculating the components of the potential gradient of the order of 0.1%, it was concluded that the central trajectory, in relation to which the time-of-flight focusing is observed, has an initial angle $\xi_0 = 90°$, i.e. it is located in the middle of the analyzed angular range of $10°-170°$. The focusing order is $N = 6$. In this case, we can only confidently say about the magnitude of the order that it is sufficiently high, i.e. time-of-flight focusing is very good. The error in calculating the time-of-flight focus position (the center s of the capacitor) was less than 5%.

The second test example demonstrates the capabilities of the proposed method in analyzing the quality of time-of-flight focusing, which is mathematically expressed by the focusing ordering, in a system with a complex electrode configuration, for which an analytical solution is hardly possible, or very difficult at best. This example demonstrates the feasibility of high-quality time-of-flight focusing by the initial angle in a real non-idealized system. In addition, in the simulated design, there is a unique combination of the time-of-flight focus with the spatial angular one. Figure 4 depicts the design of the axial-symmetric toroidal deflector that provides more than 20 orders of time-of-flight focusing with a central angle $\xi_0 = 59°$ and a distance between the source and collector equal to 6.25. The cross-sectional radius of the inner electrode of the toroid is 1.5, and the outer one is 3, ratio $K/V = 1$. Calculations of the dependence of the time of flight of particles on the initial angle ξ within the range of $56° - 62°$ at the established optimal mutual arrangement of the source and collector showed that the relative time spread is really small: $\Delta t/t \approx 0.8\%$. As an additional characteristic of the deflector, the fact of second-order axis-axis type angular focusing is established near the angle $\xi_0 = 59°$.

As previously mentioned, the proposed method enables establishing the conditions for time-of-flight focusing with respect to the initial angle (see above spherical mirror and toroidal deflector), initial position, and initial particle energy. In the following test examples, the paper will demonstrate the method's possibilities in the analyzing schemes with a spread of particles according to their position on the axis of symmetry (see below an immersion objective) and according to their energy (see below three-electrode electrostatic mirror).

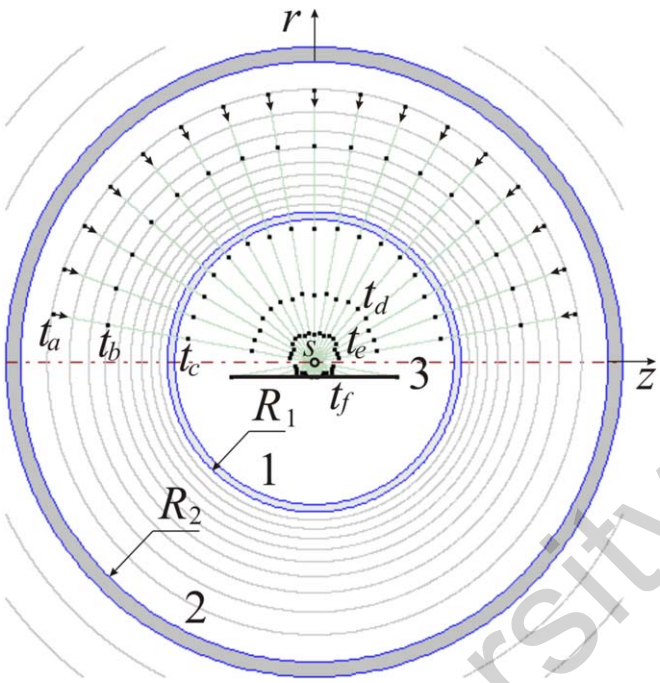

Figure 3. Search for time-of-flight focusing in a spherical capacitor.

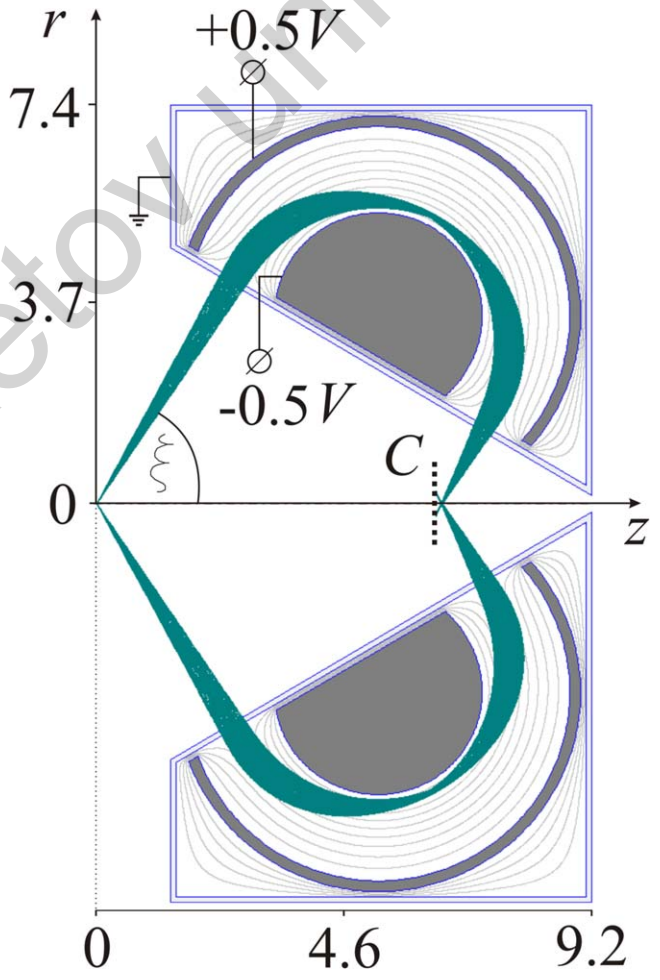

Figure 4. Search for time-of-flight focusing in a toroidal deflector with respect to the initial angle $\xi = \alpha$.

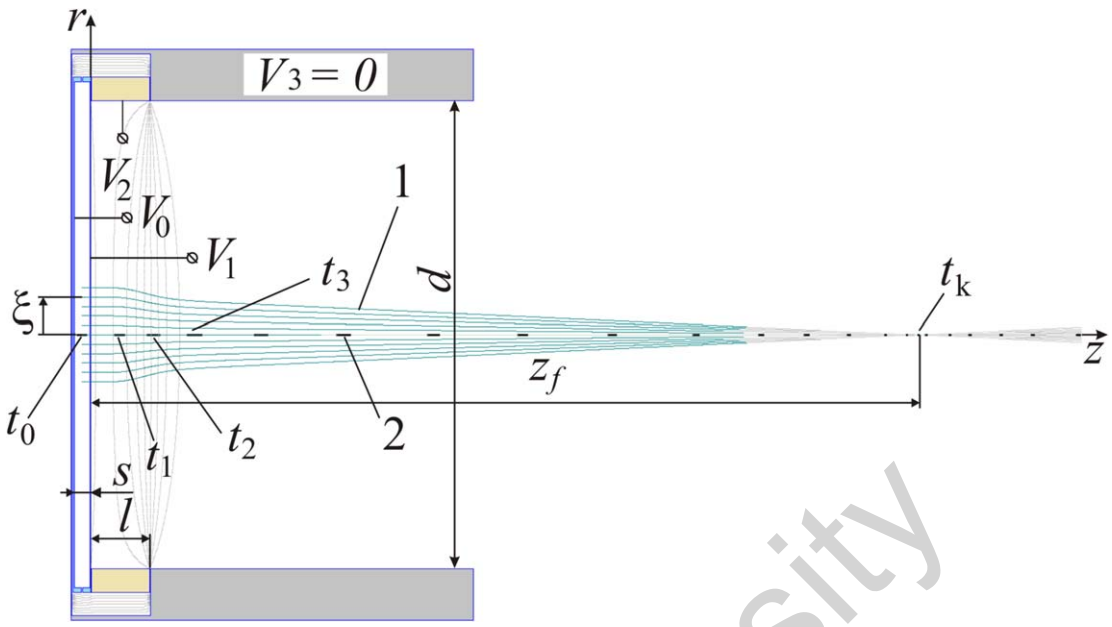

Figure 5. Time-of-flight and spatial focusing in an immersion objective.

Classical numerical methods for modeling corpuscular optics systems are ideal for solving analysis problems. Whereas the problems of synthesizing systems with new corpuscular-optical properties are solved with great success by analytical methods, in particular, methods of paraxial optics using the means of the aberration theory to eliminate or reduce the most significant aberration coefficients. In work [21], a scheme of a time-of-flight axially-symmetric mass analyzer with a straight optical axis is synthesized, in which the spatial and time-of-flight foci are combined. However, the calculated parameters of the proposed mass analyzer can be considered only approximate due to the low accuracy of paraxial methods and the analytical approximation of the axial potential distribution. Numerical analysis of the proposed scheme (figure 5) made it possible to refine the results of analytical calculations. In this case, condition of spatial focusing, i.e. in our case, the focusing of particles with different initial radii ($\xi = r_0$) was also determined numerically (see author's method [19]). The mass analyzer consists of an accelerating gap to which a pulsed expulsive voltage ($V_0 - V_1$) is applied; an exit window covered with a fine-structured metal mesh with a potential $V_1 = 1V$, and two cylinders with potentials $V_2 = 0.889$V and $V_3 = 0V$ for the case of a positive charge of the analyzed particles. The length of the cylinder with the potential V_2 is $l = 0.743d$. The size of the insulating gap between cylindrical electrodes is $0.001d$. Numerical studies show that when the distance between the electrodes is increased to $0.05d$, the changes in the calculated parameters do not exceed the limits of their calculation error. Figure 5 shows the trajectories 1 of particles emitted by a plane source and focused at a distance z_f. The source diameter is $0.2d$, where d is the inner diameter of the cylindrical electrodes. The source plane coincides with the central plane of the accelerating gap. The static trajectories of the immersion objective (figure 5) are overlaid with axial charged particle packets 2 formed at the initial moment t_0 by a source with sizes $\Delta z = 0.5s$ extended along the z -axis and fixed at different moments t_0, t_1 t_2, etc The positions of the spatial and time-of-flight foci on the z-axis depend on the value of the expulsive voltage ($V_0 - V_1$). The scheme in figure 5 provides spatial second-order focusing (with respect to the parameter $\xi = r_0$) and fourth-order time-of-flight focusing (with respect to the parameter $\xi = z_0$); it is in absolute agreement with the results of [21]. The coincidence of the positions of the corresponding foci according to the results of calculations by the proposed method is observed at the value of the accelerating pulse $V_0 =$ 1.08V, and the value of the focal length in this case is $z_f = 11.04d$, in contrast to the analytical value $z_f = 8.06d$ presented in [21]. The presented graphical results in figure 5 demonstrate the actual coincidence of the spatial and time-of-flight foci at the distance $z_f = 11.04d$ and at the time point t_k.

Here, we note the numerical method proposed in this work for searching time-of-flight focusing conditions with the previously proposed method for spatial focusing search [19], has made it possible, in fact, to solve the problem of synthesizing a scheme that combines the spatial and time-of-flight focusing conditions.

Let us demonstrate further the corpuscular-optical properties of a unique mass analyzer by numerical methods. Figure 6 shows the dynamics of a charged particle packet of the same mass with an initial diameter $d_s = 0.2d$ and an extension $\Delta z = 0.5s$ along the z-axis in the considered time-of-flight device. We note right now that the smallest packet width on the z-axis is observed at the time point t_k at a distance $z_f = 11.04d$ and coincides with the region of the smallest particle flow cross section. An analysis of the flow radial structure makes

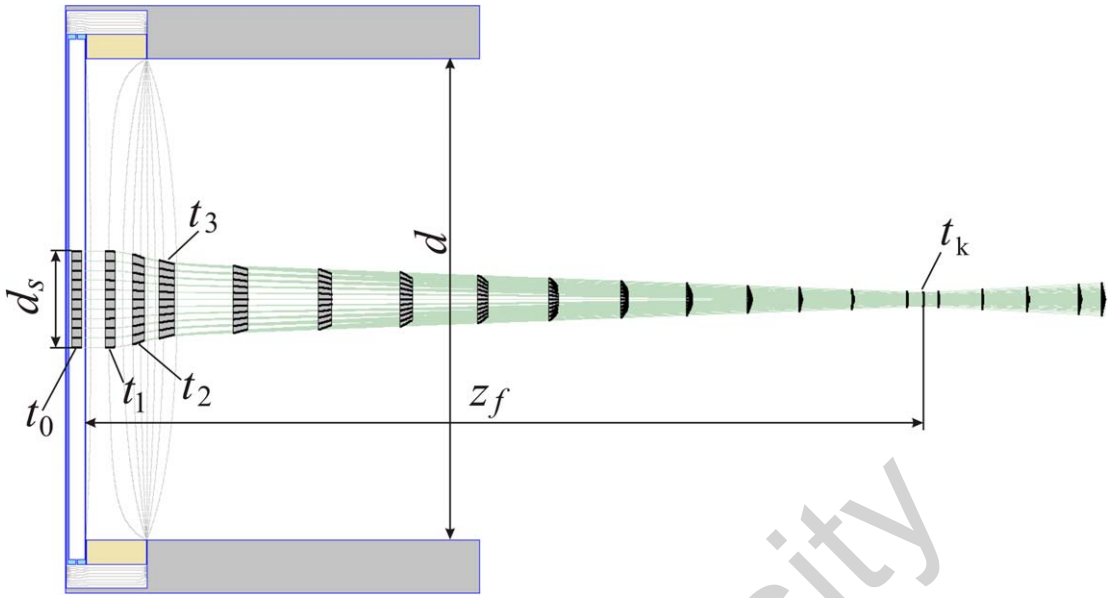

Figure 6. Movement of a wide packet of charged particles in an immersion objective.

it possible to explain the phenomenon of simultaneous time-of-flight focusing (or along the z-axis) and compression along the r -axis: the leading edge of a packet of the particles, which have lower initial energy when leaving the ionizer (accelerating gap), is more actively pressed by the lens field to the z -axis (spatial focusing) and moves along the axis more slowly (time-of-flight focusing) than particles of the trailing edge. From the analysis made it is clear, in particular, that conditions (the length of the electrodes and their potentials) for combining the spatial and time-of-flight foci can always be found for designs of this type, including using the proposed numerical method.

Figure 7 shows the process of spatial separation of ion packets of different masses $m_1 = 100$Da and $m_2 = 102$Da. The initial packet of ions, with the initial diameter $d_s = 0.04d$ and the axial extent $\Delta z = 0.5s$, after receiving energy in the accelerating gap, enters the focusing field of the immersion objective. When the packet moves in the objective field, it is gradually divided into packets with m_1 and m_2 and each of them is compressed along the z- and r-axes. Maximum compression (time-of-flight and spatial focusing) is provided at a distance of $z_f = 11.04d$. The mass resolution of the analyzer, found by the formula $R = \frac{0.5t}{\Delta t}$, is about $R = 2000$, where t is the moment when the packet reaches the collector plane placed at the distance z_f, δt is the duration of the packet when crossing the collector plane.

Due to the simplicity of the design, the considered device can be used not only as a mass analyzer, but also as a particle source with a qualitative mass pre-separation.

In [15], electrostatic mirrors of rotational symmetry with third-order time-of-flight focusing by energy were studied using the methods of paraxial optics and the theory of aberrations. The mirrors consist of three cylindrical electrodes isolated from each other by small gaps (figure 8). Various modes of mirror operation were considered in detail: the mode of focusing parallel beams, collimator and telescopic modes. As a test example, we use the results of [15] for the focusing mode of parallel beams. This mode is provided by applying the following potentials $V_1 = 1$V, $V_2 = 1.952$V, $V_3 = 2.378$V to the corresponding electrodes in case of a positive particle charge. The length of the first and third cylinders significantly exceeds their inner diameter d. The relative length of the second electrode equal to $l/d = 0.65$. The size of the isolation gaps between the electrodes is $0.001d$.

It is a fairly obvious fact that time-of-flight chromatic aberrations limit the resolving power of time-of-flight mass spectrometers, while spatial and time-of-flight geometric aberrations limit their sensitivity. One of the main properties of the proposed scheme is the combined spatial and time-of-flight foci provided that $z_T = z_F = 5.44d$, where z_T is the coordinate of the object plane, z_F is the focus position. The center of the gap between the second and third electrodes was taken as the origin along the z-axis.

The results of numerical analysis of the mirror design confirm the conclusions of work [15]. Specifically, for particles with energy $K = qV_1$ in the scheme shown in figure 8, a second-order spatial focusing with respect to the parameter $\xi = r_0$ is observed. However, the value of the spatial focus $z_F = 5.35d$ is found to be 1.5% less than expected. The third order of time-of-flight focusing in terms of the initial particle energy ($\xi = K_0$) also coincides with the order stated in [15]. In this case, the object and focal planes are similarly aligned in space at distance $z_T = z_F \approx 5.45d$ with respect to the origin of coordinates.

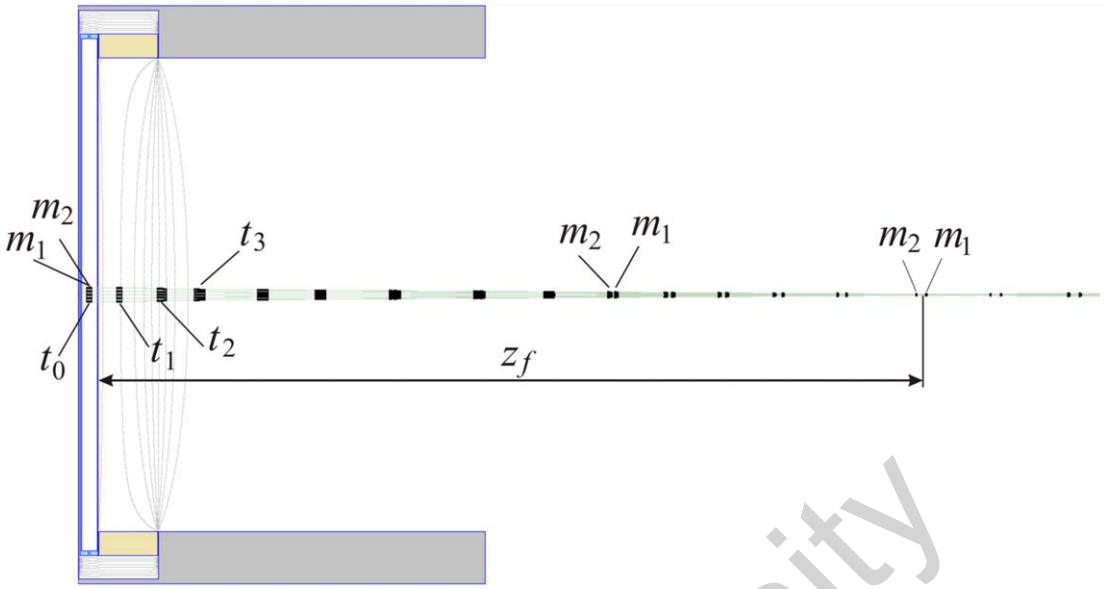

Figure 7. Movement and separation of charged particle packets with masses $m_1 = 100$ Da and $m_2 = 102$ Da.

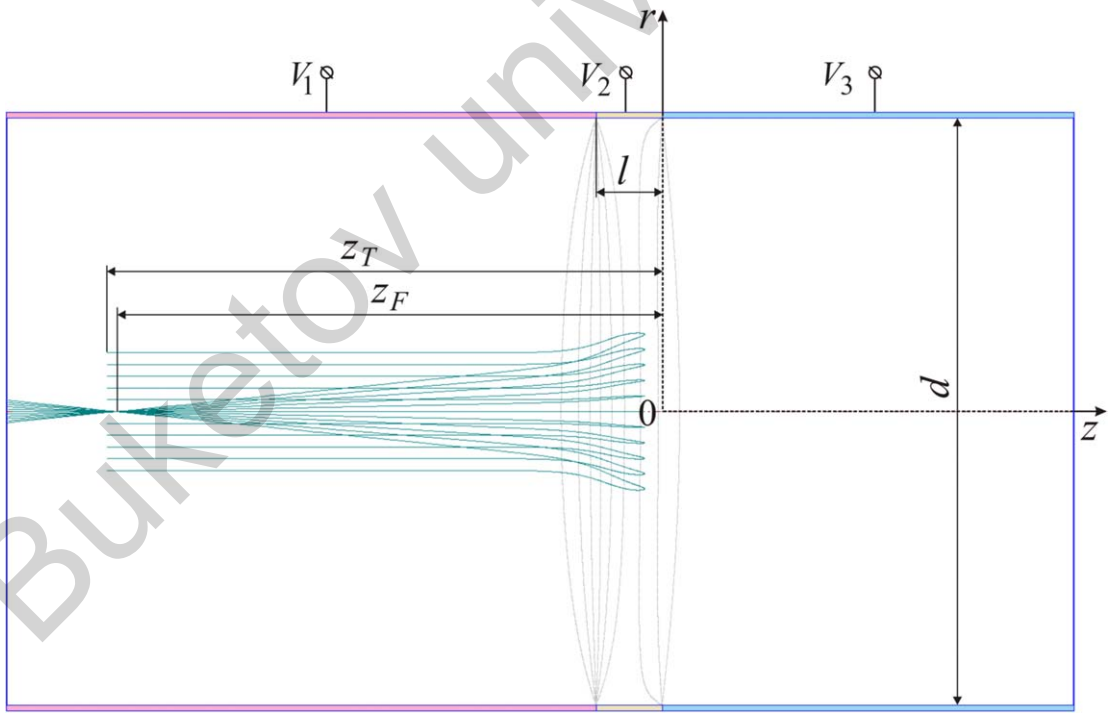

Figure 8. Spatial focusing of a parallel beam in a three-electrode electrostatic mirror with energy $K = qV_1$.

The presented above parameters of time-of-flight focusing were numerically estimated for the axial particle beam. Figure 9 demonstrates the low level of longitudinal chromatic aberrations in the focal plane of the mirror for the off-axis beam, due to the qualitative time-of-flight focusing by energy demonstrated earlier.

The figure 9 depicts three particles *s*, *a* and *h*, launched at the time moment t_0 with initial energies $K_s =$ 0.95 eV, $K_\alpha = 1.0$ eV, and $K_h = 1.05$ eV at some distance from the axis ($r_0 > 0$) from the position with coordinate $-z_T$. As the particles move towards the return point in the mirror, they move away from each other (see time moments t_1, t_2, t_3. At the time moment t_4, the direction of particle motion changes and fast particles

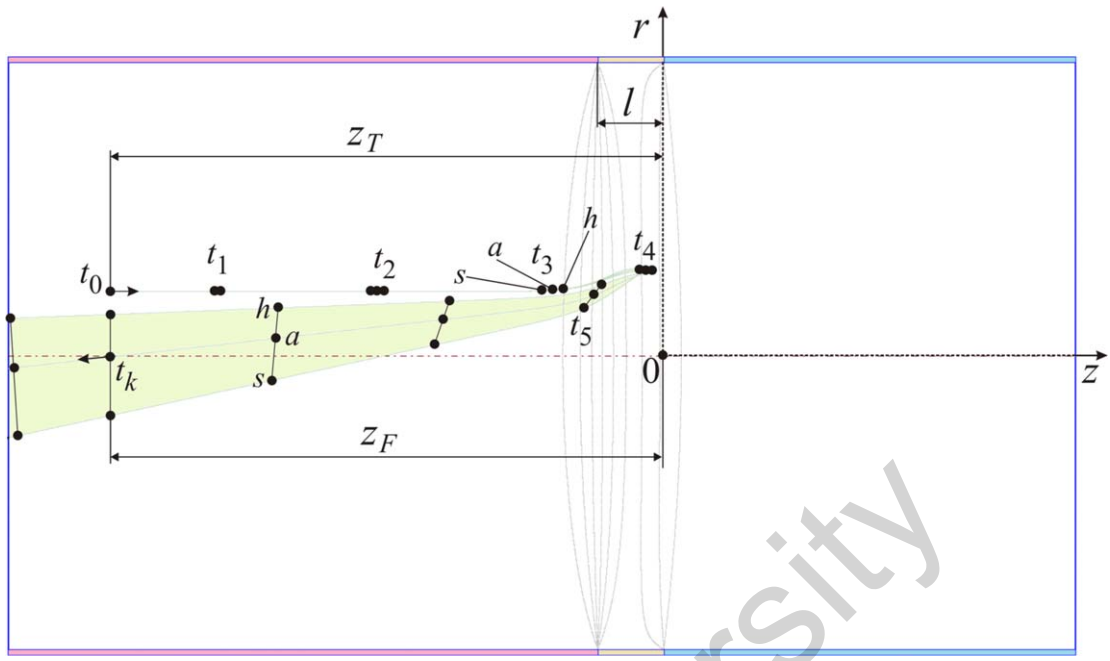

Figure 9. Time-of-flight focusing of particles s, a and h, launched with initial energies $K_s = 0.95$ eV, $K_\alpha = 1.0$ eV, $K_h = 1.05$ eV at the time moment t_0.

begin to catch up slow ones along the movement path. At the time moment t_k, particles s, a and h cross the focal plane z_F almost simultaneously.

Based on the combination of its properties, the scheme of the considered device was recommended in [15] as a highly dispersive mass reflectron. However, despite the unique corpuscular-optical properties of the scheme, when constructing a real device, the high level of transverse (along the r-axis) chromatic aberrations (see figure 9) must be taken into account, which the developers of gridless charged particle mirrors did not consider.

This article does not discuss multi-reflection time-of-flight systems, which are a natural extension of the reflectrons. The authors here set themselves the main task of demonstrating the capabilities and advantages of a new method for designing time-of-flight mass analyzers. However, the authors are planning numerical studies of advanced time-of-flight systems, including multi-reflection time-of-flight ones, in particular, the device described in [22], using the proposed numerical approach of search for time-of-flight focusing conditions. The technique can be adapted to solve this type of problem since the counting stop plane in which the functions $\nu(\xi_i)$ and $t_l(\xi_i)$ are fixed, is sufficient to declare transparent for particles on the required number of first reflections (turns). This variation of the method will allow one to determine the exact positions of the particle source and the detector plane, which provide a high order of time-of-flight focusing after any number of reflections. Additionally, it will establish the fact of migration of the plane of time-of-flight focusing in the process of reflections; will make it possible to quantify the degree of improvement or deterioration of the time-of-flight focusing in a real electric field, taking into account edge effects and its other non uniformities at a significant number of revolutions.

At the conclusion of our article, we highlight that the input data for the proposed method are the results of trajectory analysis. The practice of using the method has shown that the error in the calculation of the ordering and geometrical parameters of focusing is mainly determined by the errors in finding the moment of time t_1 of the crossing of the particle with an arbitrarily chosen counting stop surface and the velocity v of the particle at this moment. Therefore, ultimately, the accuracy of determining the time-of-flight characteristics will depend on the accuracy of calculating trajectories, taking into account all the specifics of the simulated corpuscular-optical system.

Conclusion

A numerical method of searching for conditions and estimating the order of time-of-flight focusing, based on a trajectory analysis of systems of charged particle optics, was proposed. The defined focusing conditions encompass the central value of the independent variable (source position, particle emission angle, initial energy

or velocity) in relation to which focusing occurs, as well as the position of the focus itself. The method was tested on model problems and on problems with known solutions. The main conclusions are confirmed and the results of studies carried out in the paraxial approximation and concerning the synthesis of schemes with combined high-order time-of-flight and spatial foci are refined.

Acknowledgments

The authors are grateful to Professor Bimurzaev S.B. for the formulation of the problem. The research was supported by the Ministry of Science and Higher Education of the Republic of Kazakhstan, Grant number AP09058188.

Data availability statement

All data that support the findings of this study are included within the article (and any supplementary files).

ORCID iDs

Zhanar Kambarova https://orcid.org/0000-0001-9808-5484
Arman Saulebekov https://orcid.org/0000-0002-6842-9263
Andrey Trubitsyn https://orcid.org/0000-0002-9337-8947

References

[1] de Hoffman E and Stroobant V 2007 *Mass Spectrometry: Principles and Applications* (John Wiley & Sons, Ltd) *West Sussex PO19 8SQ*
[2] Lebedev G *et al* 2007 Complete momentum and energy resolved TOF electron spectrometer for time-resolved photoemission spectroscopy *Nucl. Instrum. Meth. Phys. Res.* A **582** 168–71
[3] Fulst A, Lokhov A, Fedkevych M, Steinbrink N and Weinheimer C 2020 Time-focusing time-of-flight, a new method to turn a MAC-E-filter into a quasi-differential spectrometer *Eur. Phys. J.* C **80** 956
[4] Aker M *et al* 2019 Improved upper limit on the neutrino mass from a direct kinematic method by KATRIN *Phys. Rev. Lett.* **123** 221802
[5] Kambarova Z T, Saulebekov A O and Trubitsyn A A 2022 The all-sky spectrometer of hot cosmic plasma *Astron. J* **164** 47
[6] Damaschin I 1995 Ion-optical solutions in time-of-flight mass spectrometry *Rapid Commun. Mass Spectrom.* **9** 985–97
[7] Wiley W C and Mclaren I H 1955 Time-of-flight mass spectrometer with improved resolution *Rev. Sci. Instrum.* **26** 1150
[8] Picaud V *et al* 2018 Linear MALDI-ToF simultaneous spectrum deconvolution and baseline removal *BMC Bioinf.* **19** 1–20
[9] Yıldırım M *et al* 2010 Designing multi-field linear time-of-flight mass spectrometers with higher-order space focusing *Int. J. Mass spectrom.* **291** 1–12
[10] Mamyrin B A, Karataev V I, Shmikk D V and Zagulin V A 1973 The mass-reflectron, a new nonmagnetic time-of-flight mass spectrometer with high resolution *Sov. Phys. - JETP* **37** 45–8
[11] Handa T, Horio T, Arakawa M and Terasaki A 2020 Improvement of reflectron time-of-flight mass spectrometer for better convergence of ion beam *Int. J. Mass spectrom.* **451** 116311
[12] Moskovets E V 1991 Optimization of the reflecting system parameters in the mass-reflectron *Appl. Phys.* B **53** 253–9
[13] Berger C 1983 Compensator role of the electrostatic mirror in time of flight mass spectrometry *Int. J. Mass Spectrom. Ion Phys.* **46** 63–6
[14] Bimurzaev S B, Daumenov T, Sekunova L M and Yakushev E M 1983 Spatial-time-of-flight focusing in a two-electrode electrostatic mirror *Sov Phys.-Tech. Phys.* **28** 326
[15] Bimurzaev S B, Aldiyarov N U and Sautbekova Z S 2020 High dispersive electrostatic mirrors of rotational symmetry with the third order time-of-flight focusing by energy *Tech. Phys.* **65** 1150–5
[16] Agilent Company website August 2023 Description of Quadrupole Time of Flight Instrument of liquid chromatography/mass spectrometry. (https://agilent.com/en/product/liquid-chromatography–mass-spectrometry-lc-ms/lc-ms-instruments/quadrupole-time-of-flight-lc-ms/6530-q-tof-lc-ms)
[17] Yavor M 2009 *Optics of Charged Particle Analyzers* (Elsevier) p 381
[18] Wollnik H 1987 *Optics of Charged Particles* (Academic) p 293
[19] Gurov V S, Saulebekov A O and Trubitsyn A A 2015 Analytical, approximate-analytical and numerical methods in the design of energy analyzers *Advances in Imaging and Electron Physics* ed P.W. Hawkes (London: Academic Press) p 209
[20] Trubitsyn A, Grachev E, Gurov V, Bochkov I and Bochkov V 2017 CAE 'FOCUS' for modelling and simulating electron optics systems: development and application *Proc. SPIE* **10250** 102500V-1–102500V-7
[21] Bimurzaev S B 2015 A TOF mass spectrometer with higher resolution and sensitivity via elimination of chromatic TOF aberrations of higher orders *Int. J. Mass spectrom.* **376** 23–6
[22] Yavor M, Plaß W R, Geißel H and Scheidenberger C 2015 Ion-optical design of a high-performance multiple-reflection time-of-flight mass spectrometer and isobar separator *Int. J. Mass spectrom.* **381-382** 1–9